

Natural Correlation Diagrams. A Unifying Theoretical Basis for Analysis of n Orbital Initiated Ketone Photoreactions

Bernard Bigot,* Alain Devaquet, and Nicholas J. Turro*

Contribution from the Laboratoire de Chimie Organique Théorique, Université Pierre et Marie Curie, Tour 44-45, 4 Place Jussieu, Paris Cedex 75230, France, and Chemistry Department, Columbia University, New York, New York 10027. Received February 6, 1980

Abstract: The four experimentally significant n orbital initiated reactions of ketones—hydrogen atom abstraction, cycloaddition to ethylenes, α -cleavage, and electron transfer—are analyzed theoretically in a unified manner starting with “natural” orbital correlations. This procedure allows similarities in the surface descriptions of these reactions to become apparent. It is shown that the primary photochemical reactions of ketones in their n,π^* states are fundamentally of two conceptually distinct types: those which involve the formation of a new σ bond to the ketone and those which rupture a σ bond possessed by the ketone. The role of charge-transfer states in modifying photoreaction pathways is discussed.

Avoiding Crossings at the MO Level. Natural Correlation Diagrams

Correlation diagrams have been of great assistance in the analysis of both photochemical and photophysical processes.¹ Adiabatic state correlation diagrams have been particularly useful for the qualitative recognition of reaction pathways (“reactive channels”) that are available to the array of electronically excited states of an initial system of reactants. However, as will be discussed below, qualitative adiabatic correlations at the state level fail to reveal the (often small) barriers that arise on potential energy curves (PEC’s) as a result of avoided crossings which occur at the MO stage of a correlation. The term “natural” correlations has been suggested to describe the PEC’s that arise from MO avoided crossings.² The natural correlations differ from the classical Woodward–Hoffmann^{3a} or Salem state^{3b} correlations in two important features. First, the natural correlations of MO’s are based on the conservation of phase relations and of local electronic distributions in addition to the classical conservation of overall state symmetry properties relative to selected local symmetry elements. Second, in the natural correlation diagram two “correlation lines” associated with MO’s of the same symmetry are allowed to cross, in order to identify the intended correlations. These intended correlations may provide important insight to the source of small energy barriers or energy wells because they indicate “where the MO’s wish to go” before symmetry avoided crossings are considered and before the state diagram is constructed.

The results of numerous experimental investigations of photochemical reactions over the past decade have demonstrated that small energy barriers (~ 3 – 10 kcal/mol)⁴ indeed do exist between initial electronically excited states and primary reaction intermediates. It seems likely that a significant fraction of the experimental energy barriers may be associated with the avoided crossings that arise in state correlation as the memories of the natural correlation, and, if this is so, it becomes important to be able to predict the existence of such energy barriers.

State Correlation Diagrams. Electronically Allowed and Electronically Forbidden Photoreactions. Let us now define the notations in the final state correlation diagrams. A straight line between the two states means that the correlation between these states is direct. A direct correlation means that there is no electronically imposed energy maximum or energy well on the potential energy curve which links the two corresponding states. A curved line between two states means that the correlation between these states results from an (or several) avoided crossing(s) somewhere between the starting species and the finally formed state.

Electronically, Thermodynamically and Kinetically Allowed Photoreactions. Two types of data have to be considered in the discussion of the final state correlation diagram. One type is relevant to the electronic properties and the other to the thermodynamic properties of the initial and final states under scrutiny. A reaction pathway from an initial state of the starting system may be electronically allowed or forbidden. A reaction is electronically allowed if the initial state correlates directly with the ground state of the first formed intermediate. A reaction is electronically forbidden if the initial state correlates with an excited state of the first formed intermediate. Of course, even for the latter case, the ground state of the intermediate might be reached via internal conversion, intersystem crossing, or a series of non-radiative decays.

By analogy to the concept of electronic allowedness or forbiddenness as defined in terms of correlation diagrams, thermochemical allowedness or forbiddenness may be defined in terms of whether the product state is energetically disposed above (endothermic reaction) or below (exothermic reaction) the starting state (Figure 1). It also should be noted that the thermochemical criterion does not explicitly consider entropy effects. Thus, in bimolecular reactions the theoretical discussion must refer to experimental conditions that are pseudo-first order (i.e., the ground-state substrate is in large excess) and to reactions for which entropic factors are not rate determining.

Electronic and thermochemical “allowedness” are “static” properties of a correlation diagram; i.e., feasibility is indicated. The experimentalist wishes to identify an “allowed” reaction with a reaction that is *efficient* under a given set of reaction conditions. In photoreactions the pertinent efficiency is given by the fraction of initial excited states that undergo a reaction of interest. This fraction is the state quantum yield for reaction, ϕ_r , and is given by eq 1, where k_r is the first-order (or pseudo-first-order) rate

$$\phi_r = \alpha k_r \tau \quad (1)$$

constant for reaction, τ is the lifetime of the reactive state, and α is the efficiency of formation of the excited state per photon absorbed by the system.

With the assumption that k_r follows an Arrhenius behavior,

$$\phi_r = \alpha \tau A \exp(-E_a/RT) \quad (2)$$

(1) (a) J. Michl, *Mol. Photochem.*, **4**, 243, 257 (1972); J. Michl, *Top. Curr. Chem.*, **46**, 1 (1974). (b) A. Devaquet, *Pure Appl. Chem.*, **41**, 455 (1975); *Top. Curr. Chem.*, **54**, 1 (1975). (c) N. D. Epiotis and S. Shaik, *Prog. Theor. Org. Chem.*, **2**, 348 (1977).

(2) (a) A. Devaquet, A. Sevin, and B. Bigot, *J. Am. Chem. Soc.*, **100**, 2009 (1978). (b) B. Bigot, A. Sevin, and A. Devaquet, *ibid.*, **101**, 1095 (1979), and references therein. (c) B. Bigot, Ph.D. Thesis, Université Pierre et Marie Curie, June 1979. (d) For previous analogous approaches to the correlations discussed here see: H. E. Zimmerman, *J. Am. Chem. Soc.*, **88**, 1563, 1564 (1966); W. A. Goddard, *ibid.*, **94**, 793 (1972).

(3) (a) R. B. Woodward and R. Hoffmann, “The Conservation of Orbital Symmetry”; Academic Press, New York, 1970. (b) L. Salem, *J. Am. Chem. Soc.*, **96**, 3486 (1974); W. G. Dauben, L. Salem, and N. J. Turro, *Acc. Chem. Res.*, **8**, 41 (1975).

(4) For a discussion see: N. J. Turro, “Modern Molecular Photochemistry”; Benjamin/Cummings, Menlo Park, CA, 1978; p 235.

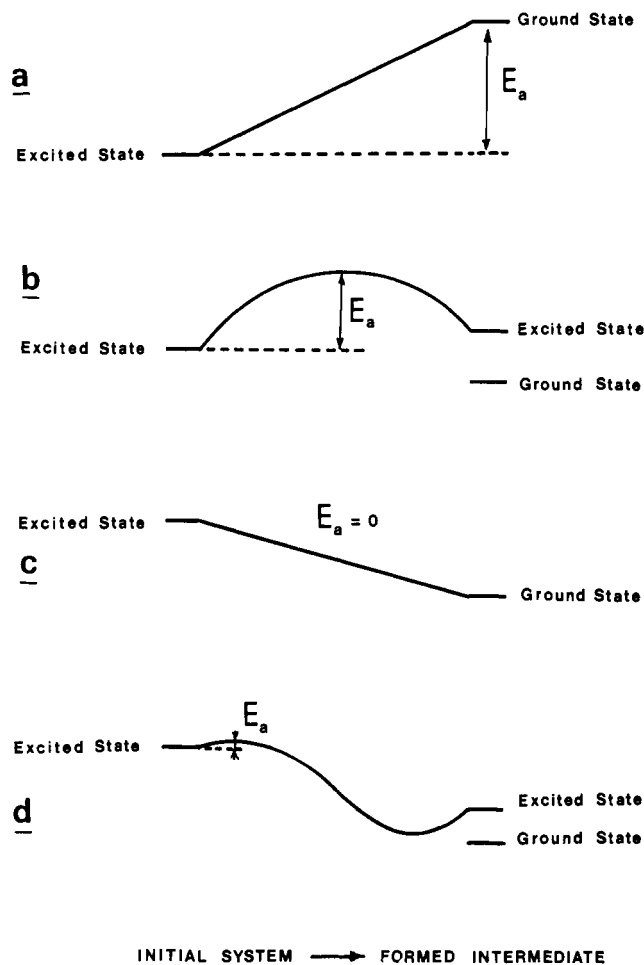


Figure 1. Various examples of potential energy curves illustrating the electronically-thermodynamically allowedness or forbiddenness starting from a given excited states: (a) electronically allowed, thermodynamically forbidden; (b) electronically forbidden, thermodynamically forbidden; (c) electronically allowed, thermodynamically allowed; (d) electronically forbidden, thermodynamically allowed.

Since efficiencies of reaction are the experimentally pertinent quantities and yet since theoretical correlation diagrams refer to k_r , any serious comparison of theory with experiments must recognize the role of the excited-state lifetime τ and its efficiency of formation α , the A factor, the activation energy E_a , and the reaction temperature T .

In the following discussion, we shall suppress explicit consideration of α , A , and T , since these may be handled straightforwardly in each individual case. We wish to point out, however, that experimentally "allowed" photoreactions are those that occur with high efficiency from a given state, i.e., those reactions for which the activation energy E_a can be readily achieved during the excited-state lifetime, τ .

Thus, in addition to the theoretically useful and clearly defined concept of *electronically (thermochemically) allowed* or *electronically (thermochemically) forbidden reactions*, one must consider the concept of *kinetically allowed* or *kinetically forbidden reactions* which refer to a specific set of experimental conditions.⁴ It is instructive to identify two separate factors which contribute to E_a : thermochemical factors which simply have to do with the energetics of the initial and final state and which are independent of reaction pathway, and electronic factors which relate to barriers and minima imposed by surface crossings or surface avoidings. In terms of conventional surface diagrams, if a state correlation line is straight but if the final state lies at a higher energy than the initial state, the reaction is unambiguously electronically allowed but will possess an activation energy E_a equal to the reaction endothermicity (Figure 1). If E_a is large enough, $k_r\tau \ll 1$ and the reaction is electronically allowed but kinetically

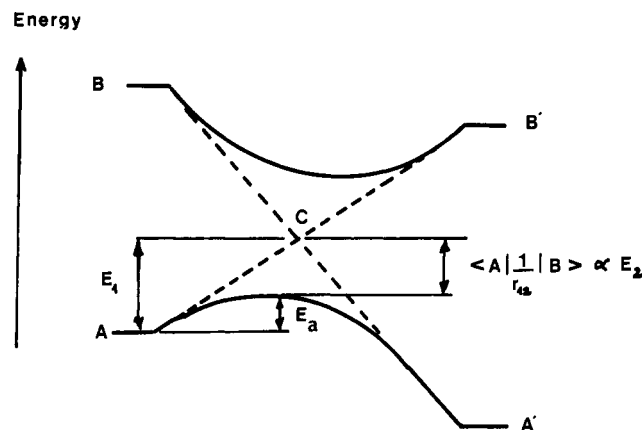


Figure 2. Schematic representation of an avoided crossing.

forbidden. In some cases (Figure 1) an activation energy above and beyond that due to reaction endothermicity may serve to further decrease $k_r\tau$.

The original Salem diagrams^{3b} referred to adiabatic rather than natural correlation connections between initial and primary product states in photoreactions. Such an attitude does not explicitly consider barriers due to natural correlations which eventuate in avoided crossings. Only when such barriers are small enough to be surmounted readily during the lifetime of the excited state will the reaction be "kinetically allowed".

One important goal of correlation diagrams is to qualitatively estimate E_a for thermodynamically allowed—electronically allowed reactions for which a barrier results from an avoided crossing. The magnitude of E_a is determined by the difference between two terms E_1 and E_2 (see Figure 2). E_1 is the energy difference between the position of the starting state and the position of the crossing point C. E_2 is the term $\langle A | \frac{1}{r_{12}} | B \rangle$ —which represents the avoiding between the two configurations A and B which the correlation lines intend to cross. E_a is smaller when E_1 is small and E_2 is large. E_1 is small when B and B' are low-lying excited states, and E_2 is large when A and B differ by less than two spin-orbitals which have good overlaps.⁵

The Salem adiabatic correlation scheme has been successful in spite of the neglect of barriers imposed by natural correlations. This means that such barriers are small, if they exist at all. It may be that if a photoreaction is adiabatic and thermochemically allowed from the initial state to the primary product state, that the "density of surface crossings" in the phase space of excited states will generally guarantee avoidings that will destroy the natural correlation and cause only low barriers on the adiabatic pathway to product.

n Orbital Initiated Reactions of Ketones. The reactions of the n, π^* states of ketones are known to be relatively insensitive to spin multiplicity and are dominated by the electrophilic character of the half-filled n orbital.⁶ Four photoreactions of ketones are generally initiated by overlap with the half-filled n orbital: (1) hydrogen atom abstraction; (2) α cleavage; (3) cycloaddition to olefins; (4) electron transfer from electron donors such as amines. The primary photochemical step for each of these reactions is shown schematically in terms of standard Lewis Structures in Figure 3. We will show that the first three reactions can be analyzed in a parallel fashion and that the electron-transfer reaction from amines can be considered as a simple variation of the first three reactions.

MO Pattern for the n-Initiated Hydrogen Abstraction, α Cleavage, and Olefin Addition of Ketones. The main MO's of the initial system concerned in the hydrogen abstraction by ketones are the σ_{CH} -bonding and σ^*_{CH} -antibonding orbitals of the CH bond of RH which will be broken during the reaction, the n_O lone-pair orbital of the oxygen atom, and the π_{CO} -bonding and π^*_{CO} -an-

(5) L. Salem, C. Leforestier, G. Segal, and R. Wetmore, *J. Am. Chem. Soc.*, **97**, 679 (1975).

(6) Reference 4, p 219.

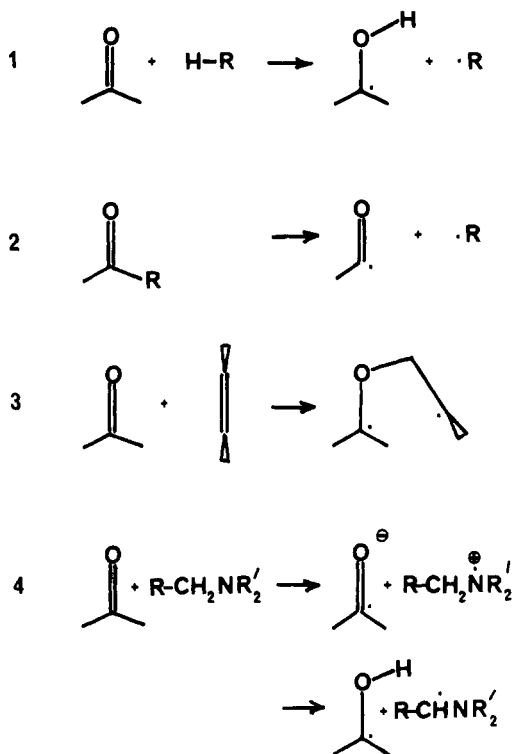


Figure 3. *n*-Initiated ketone reactions: 1, hydrogen abstraction from alkyl group; 2, α cleavage; 3, olefin addition; 4, electron transfer from amines followed by β -hydrogen abstraction.

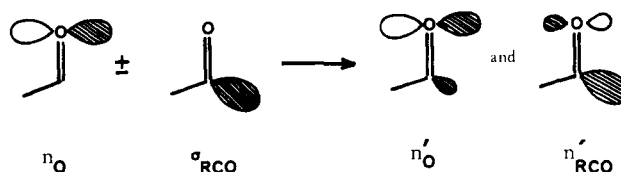
tibonding orbitals of the CO chromophore. The main MO's of the formed intermediate to be considered are the σ_{OH} -bonding and σ^*_{OH} -antibonding orbitals of the OH bond of the ketyl radical, the n_R lone-pair orbital of the carbon atom of the alkyl group, and the π orbitals already mentioned for the initial system. The natural correlations are straightforward and are shown in Figure 4. For the α -cleavage reaction, the pattern of MO's of the starting system is entirely similar to that for hydrogen abstraction reaction if one considers that the σ_{CC} and σ^*_{CC} orbitals of the CC broken bond correspond to and have energy of the same order of magnitude as the σ_{CH} and σ^*_{CH} orbitals, respectively. For the intermediate formed by α cleavage, three MO's (π_{CO} , π_R , π^*_{CO}) of the initial system are identical with those for hydrogen abstraction. The two others (n'_O and n'_{RCO}), which result from the

Table I

molecular orbital labelings	nature of the reactions		
	hydrogen abstractn	α cleavage	olefin additn
a	σ_{CH}	σ_{CC}	π_{CC}^a
b	π_{CO}	π_{CO}	π_{CO}
c	n_O	n_O	n_O
d	π^*_{CO}	π^*_{CO}	$\pi^*_{CO}^a$
e	σ^*_{CH}	σ^*_{CC}	π^*_{CC}
c'	σ_{OH}	n'_O^b	σ_{CO}
b'	π_{CO}	π_{CO}	π_{CO}
a'	n_R	n_R	n_R
d'	π^*_{CO}	$\pi^*_{CO}^b$	π^*_{CO}
e'	σ^*_{OH}	n'_{RCO}	σ^*_{CO}

^a The braces mean possible energetic inversion of the respective positions of both MO's. ^b The arrows mean inversion of the respective positions of both MO's.

in- and out-of-phase mixing of n_O and σ_{RCO} , are the counterpart of the σ_{OH} and σ^*_{OH} orbitals. But, in the α cleavage the energy gap between them is much reduced compared to the gap in the hydrogen abstraction such that n'_O is now above π_{CO} and n'_{RCO} is below π^*_{CO} . Thus the MO natural correlation diagram for



α -cleavage reaction can be deduced from that for hydrogen abstraction simply by modifying the slopes of the correlation lines starting from n_O and σ_{CH} in a qualitative manner (see Figure 4).

For olefin addition, it is the pattern of MO's of the final system which is entirely similar to that for hydrogen abstraction if one considers that the π_{CO} and π^*_{CO} orbitals of the newly formed CO bond correspond to and have energy of the same order of magnitude of the σ_{CH} and σ^*_{CH} orbitals. For the initial system, three MO's (π_{CO} , n_O , π^*_{CO}) are identical with those for hydrogen abstraction. The two other (π_{CC} , π^*_{CC}) differ from the σ_{CH} and σ^*_{CH} parent orbitals in the hydrogen abstraction by the reduced energy gap that separates them. Let us note that the relative positions of π_{CC} and π_{CO} on the one hand and π^*_{CC} and π^*_{CO} on the other hand depend on the nature (electron-rich or electron-poor) of the olefin. Thus, the MO natural correlation diagram for olefin addition can also be deduced from that for hydrogen abstraction

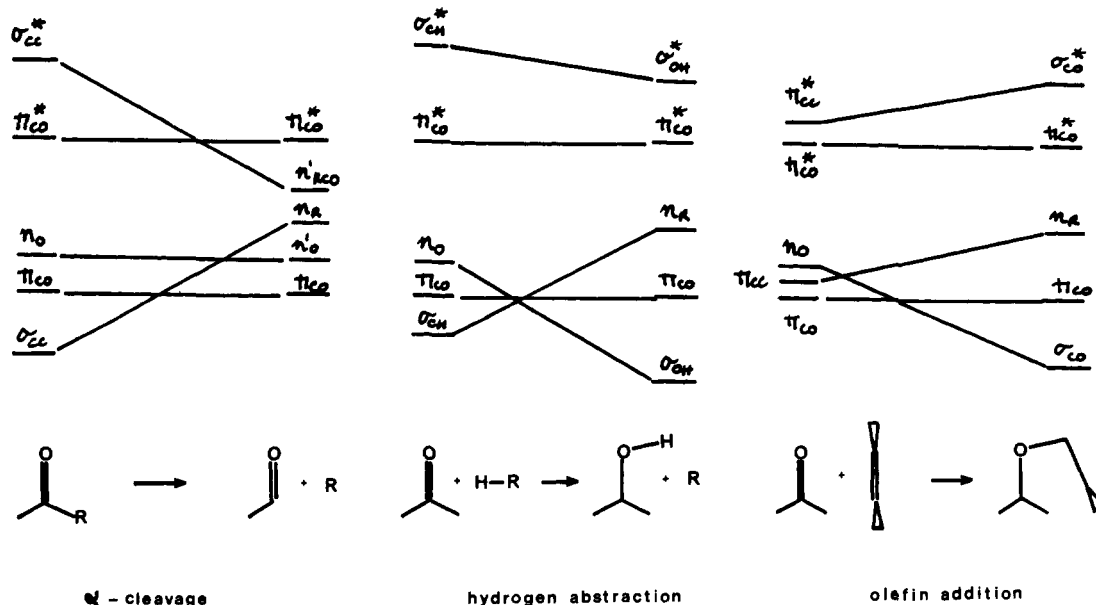
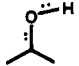

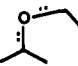
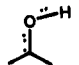
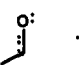
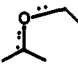
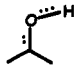
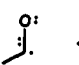
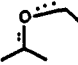
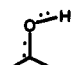

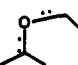
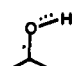
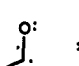
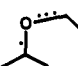
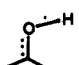

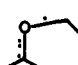
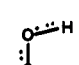

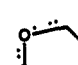
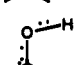
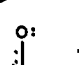
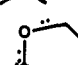


Figure 4. Natural molecular orbital correlation diagrams for α -cleavage, hydrogen abstraction, and olefin addition reactions.

Table II

Electronic Configurations	Hydrogen Abstraction	α -cleavage	Olefin Addition
<u>$a^2 b^2 c^2$</u>	$1G_s$	—	—
$c \rightarrow d$	$1,3n_o\pi^*CO$	—	—
$b \rightarrow d$	$1,3\pi_{CO}\pi^*CO$	—	—
$a \rightarrow d$	$1,3\sigma_{CH}\pi^*CO$	$1,3\sigma_{CC}\pi^*CO$	$1,3\pi_{CC}\pi^*CO$
$c \rightarrow e$	$1,3n_o\sigma^*CH$	$1,3n_o\sigma^*CC$	$1,3n_o\pi^*CC$
$b \rightarrow e$	$1,3\pi_{CO}\sigma^*CH$	$1,3\pi_{CO}\sigma^*CC$	$1,3\pi_{CO}\pi^*CC$
$a \rightarrow e$	$1,3\sigma_{CH}\sigma^*CH$	$1,3\sigma_{CC}\sigma^*CC$	$1,3\pi_{CC}\pi^*CC$
<u>$a^2 b^2 c^2$</u> $1Z$			
$a' \rightarrow d'$ $1,3D_{\sigma\pi}$			
$a' \rightarrow e'$ $1,3D_{\sigma\sigma}$			
$b' \rightarrow d'$ $1,3Z_{\pi\pi}^*$			
$b' \rightarrow e'$ $1,3Z_{\sigma\pi}^*$			
$c' \rightarrow d'$ $1,3Z_{\sigma\pi}^*$			
$(a' \rightarrow e')$ $(c' \rightarrow e')$ $1,3D_{\sigma\sigma}'$			
$(a' \rightarrow d')$ $(b' \rightarrow d')$ $1,3D_{\sigma\pi}'$			

simply on modifying the slopes of the correlation lines ending to n_R and σ_{OH}^* (see Figure 4). It follows from the preceding analysis that the three reactions under scrutiny could be studied in a unifying manner by labeling the various MO's involved in hydrogen abstraction and their counterparts of the parent reactions (a, b, c, d, e) for the starting system and (a', b', c', d', e') for the formed intermediate (see Table I). Thus, the correlations are a-a', b-b', c-c', d-d', and e-e', whatever the relative energetic position of these different MO's. Furthermore, the primary natural correlation diagrams are equivalent in the three cases. It is the relative energetic positions of the electronic states involved which determine the final aspect of the complete state diagram and the kinetically feasible surface pathways.

The electronic states of the intermediates formed in reactions of n, π^* states can be classified in two groups—the diradical states and the zwitterionic states.^{3b} The former do not involve charge separation whereas the latter do. The lowest excited states of the initial or final system are mainly monoexcited states. In exceptional cases they are doubly excited states. These states are summarized and depicted in Table II. They have been divided in two groups by energy: those whose energy is less than 250 kcal/mol above the ground state of the starting species and those whose energies are greater than 250 kcal/mol above the ground state. The states of the first group are underlined.

We note immediately from Table II that, except for certain states in the olefin addition, the lowest excited states of the initial system ($1,3n_o\pi^*CO$, $1,3\pi_{CO}\pi^*CO$) or of the final system ($1,3D_{\sigma\pi}$, $1,3D_{\sigma\sigma}$) correlate with high-lying excited states. This means that no direct correlation between the lowest excited states of the initial and final systems will occur. Thus, the reactivity of these excited states (at a given temperature) will be strongly dependent on the magnitude of the correlation imposed potential energy barrier.

If one considers the relative energy positions of the lowest potentially reactive excited states of the three reactions of Figure 4 (Table III), one observes that although numerous possible situations exist, each can be analyzed as variations of only two basic correlation diagrams. In both basic cases, one supposes that the lowest excited states of the initial system are the $1,3n_o\pi^*CO$ pair, the $3\pi_{CO}\pi^*CO$ state, and the corresponding singlet in the usual increasing energy order. The gap between the singlet and triplet $\pi_{CO}\pi^*CO$ states is assumed to be at least 5–10 times larger than the gap between the $1,3n_o\pi^*CO$ pair and the $3\pi_{CO}\pi^*CO$ state. In the first case one considers that the “ground state” of the initially formed intermediate is the degenerate $1,3D_{\sigma\pi}$ pair and that the “first excited state” is the $1Z$ state. In the second case, one considers that the ground state of the intermediate is the $1,3D_{\sigma\sigma}$ pair. Moreover, in order for the reaction to be thermodynamically allowed, it is assumed that the ground state of the intermediate is degenerate or lower in energy than the lowest excited state of the starting species. The resulting two basic diagrams are drawn in Figures 5 and 6.

First, let us consider the basic diagram of Figure 5. This diagram corresponds to a very common situation for hydrogen abstraction and olefin addition. The only low-energy reactive channels proceed from the $1,3n_o\pi^*CO$ states. They are never electronically allowed but are kinetically allowed only if the energy barriers of their PEC's are sufficiently small. The energy barrier is smaller as the energy gap between the $n_o\pi^*CO$ and the $Z_{\sigma\pi}^*$ and (a → d) states is reduced. This effect results in an increase of the polarity of the reactivity and serves to increase the reactivity of the $n_o\pi^*CO$ states since the $Z_{\sigma\pi}^*$ and (a → d) states are charge-transfer states. In hydrogen abstraction a decrease in bond strength of the donor entity (RH) favors the reaction by lowering the energetic position of the $D_{\sigma\pi}$ states.⁷ For the same reasons, in olefin addition, radical-stabilizing substituents on the β carbon of the olefin favor the reaction.⁸

Several variations of this general scheme may be considered. First of all, symmetric states can be situated below the $1,3n_o\pi^*CO$ pair, i.e., the triplet $\pi_{CO}\pi^*CO$ for olefin addition or hydrogen abstraction and the charge-transfer triplet $n_o\pi^*CC$ for olefin addition. The charge-transfer states are generally not starting points of new possible reactive channels, because they cannot be populated directly (the involved transition moment is zero with all the valence states). They intervene only on modifying the reactivity pattern by the crossing of their correlation lines with those of the valence states.

Thus, the existence of low-lying $n_o\pi^*CC$ states does not modify the general scheme. In the case of a low-lying valence $\pi_{CO}\pi^*CO$ state, this symmetric triplet has to be considered as a new potentially reactive channel. Indeed the system could jump from the surface starting from this state to the $1,3n_o\pi^*CO-1,3D_{\sigma\pi}$ surfaces via intersystem crossing or internal conversion in point C or C' (Figure 5a). Other realistic variations have to be considered with antisymmetric states below the $n_o\pi^*CO$ states. The situation could occur in olefin addition. Indeed, the charge-transfer states $\pi_{CC}\pi^*CO$ for electron-rich olefins and $\pi_{CO}\pi^*CC$ for electron-poor olefins can be situated in the vicinity or even below the $n_o\pi^*CO$ states. The situation when the $\pi_{CC}\pi^*CO$ states are below the $n_o\pi^*CO$ states brings a noticeable modification to the general scheme since these charge transfer states correlate directly with the $1,3D_{\sigma\pi}$ states. The $n_o\pi^*CO$ states possess no electronically allowed channels. No accessible reactive excited state remains. If only the triplet charge-transfer state is below the valence states, the triplet $n_o\pi^*CO$ is not reactive, but the singlet has an increased reactivity compared to the general scheme since the $1n_o\pi^*CO-1\pi_{CO}\pi^*CO$ (a → d) gap will be small (Figure 5b). However, for large distances of separation of the reacting fragments, the charge-transfer state cannot be situated below the first valence excited states. The situation when the $\pi^*CO\pi^*CC$ states are below the $1,3n_o\pi^*CO$ pair brings the most striking change to the general scheme. Indeed, on the $1,3n_o\pi^*CO-1,3D_{\sigma\pi}$ PEC's

(7) Reference 4, p 364.

(8) Reference 8, p 437.

Table III

	hydrogen abstractn	α cleavage	olefin additn	hydrogen abstractn	α cleavage	olefin additn
increasing energy \uparrow	$-^1\pi\text{CO}\pi^*\text{CO}$	b	$-^1\pi\text{CC}\pi^*\text{CC}$	$\begin{cases} -^{1,3}\text{D}'\sigma\pi \\ -^{1,3}\text{Z}^*\pi\pi \end{cases}$	$-^{1,3}\text{D}\sigma\sigma$	$\begin{cases} -^{1,3}\text{D}'\sigma\pi \\ -^{1,3}\text{Z}^*\pi\pi \end{cases}$
	$\begin{cases} -^3\pi\text{CO}\pi^*\text{CO}^a \\ -^{1,3}\text{nO}\pi^*\text{CO} \\ -\text{GS} \end{cases}$		$\begin{cases} -^1\pi\text{CO}\pi^*\text{CO} \\ -^{1,3}\pi\text{CO}\pi^*\text{CC} \\ -^{1,3}\pi\text{CC}\pi^*\text{CO} \\ -^{1,3}\text{nO}\pi^*\text{CC} \\ -^3\pi\text{CC}\pi^*\text{CC} \\ -^3\pi\text{CO}\pi^*\text{CO} \\ -^{1,3}\text{nO}\pi^*\text{CO} \\ -\text{GS} \end{cases}$			
		initial system		$-^{1,3}\text{D}\sigma\pi$	$-^{1,3}\text{D}\sigma\sigma$	$-^{1,3}\text{D}\sigma\pi$
					final system	

^a The braces mean a possible inversion of the respective positions of the concerned states. ^b The states for α cleavage are identical with those shown for hydrogen abstraction.

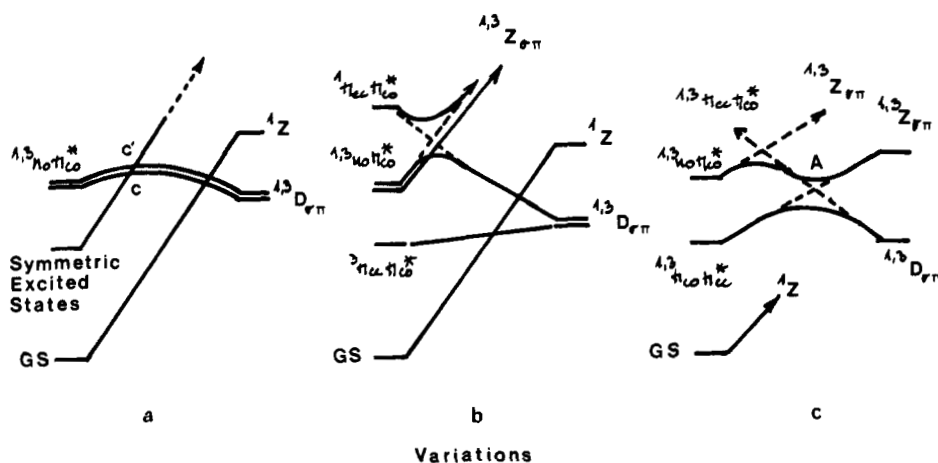
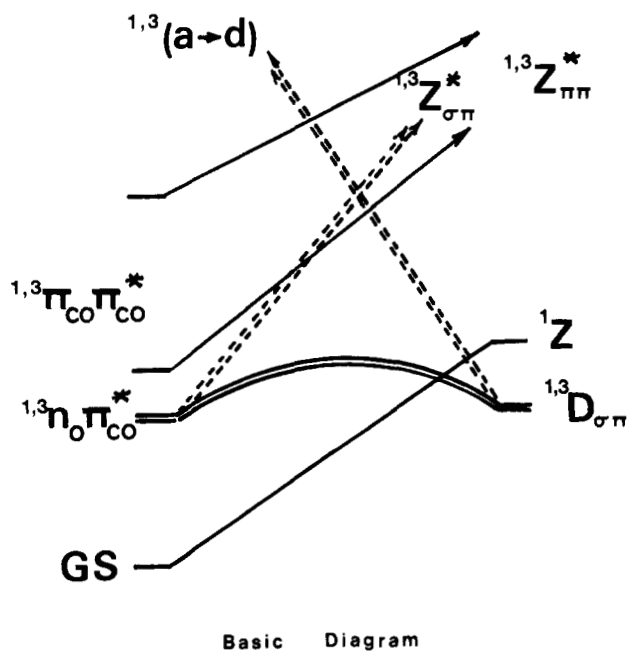
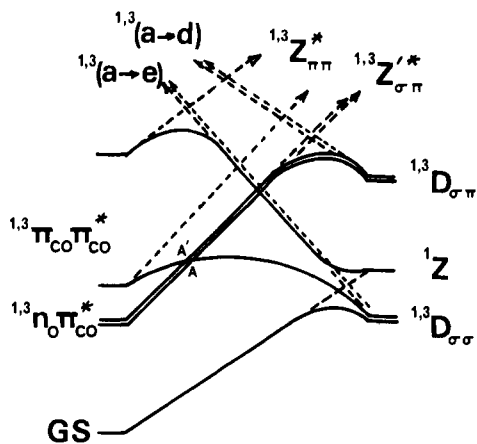


Figure 5. State correlation diagrams corresponding to the first case. From the basic diagram, the three variations 1 (a), 2 (b) and 3 (c) have been considered. The dashed lines correspond to the primary natural state correlations and the full lines to the final state correlations after consideration of the avoided crossings from symmetry reasons.

minima appear due to the supplementary avoided crossing on the correlation line which connects the $\text{D}_{\sigma\pi}$ states. These minima represent the formation of an ion-pair intermediate since it results from the crossing with a correlation line linking two charge-transfer states. Thus, in such a case, the only reactive channels remain the $\text{n}_\text{O}\pi^*\text{CO}$ states, but the reaction is now a two-step process. In a first step, there is formation of an ion pair intermediate in the

potential well A (Figure 5c). In a second step, the system decays to the lowest PEC's and leads to the formation of the diradical product. The existence of such an ionic intermediate is possible only if very low-lying charge-transfer state has to be considered. Its lifetime is longer the more strongly avoided the crossing.

For the second typical case, Figure 6 displays the various potentially reactive channels. The first one is the $^3\pi\text{CO}\pi^*\text{CO}$ state.



Basic Diagram

Figure 6. State correlation diagram corresponding to the second case. The dashed lines correspond to the primary natural state correlations.

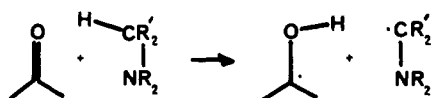
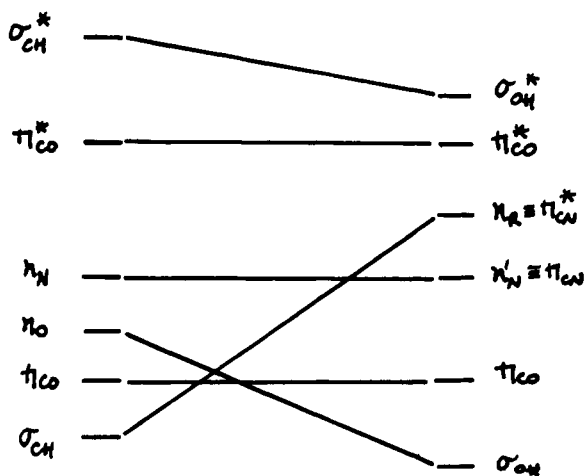


Figure 7. Natural molecular orbital correlation diagram for the electron transfer from amines followed by hydrogen abstraction.

Reaction from this state is electronically allowed, but this channel requires the overcoming of an energy barrier. A second possibility is reaction from the corresponding singlet $\pi_{CO}\pi^*_{CO}$. Here again an energy barrier must be overcome. Finally, the $1,3n_O\pi^*_{CO}$ pair can be considered as potentially reactive channels in two ways. First, if the $1,3D_{\sigma\pi}$ states are sufficiently low-lying, the direct reaction $1,3n_O\pi^*_{CO} \rightarrow 1,3D_{\sigma\pi}$ is thermodynamically allowed; from here the system decays from the $D_{\sigma\pi}$ surfaces to the lowest $D_{\sigma\sigma}$ surfaces. Second, intersystem crossing or internal conversion can occur in points A or A' and the system jumps to the $3\pi_{CO}\pi^*_{CO} \rightarrow D_{\sigma\pi}$ surface. This diagram corresponds to a general situation for α cleavage of ketones. The various realistic changes of the respective positions of the excited states do not change qualitatively the preceding conclusions.

In conclusion, the three *n*-initiated reactions of ketones, in the most common cases, involve direct formation of a diradical intermediate throughout a single potential energy surface which may require passage over an energy barrier.⁹ In other cases they may involve formation of an intermediate with ion-pair character.

MO Pattern for Electron Transfer from Amines. Let us now consider the hydrogen abstraction from amines. This reaction

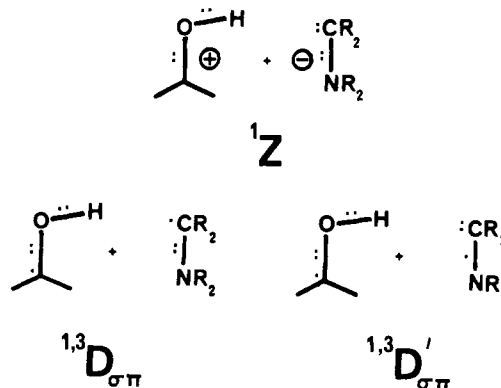


Figure 8. Schematic description of the lowest electronic states of the formed intermediate in the hydrogen abstraction from electron-donor species.

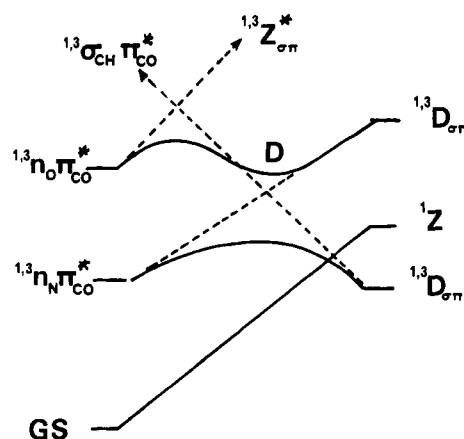
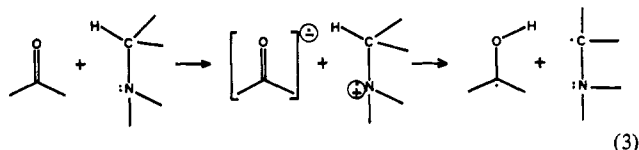


Figure 9. State correlation diagram for the hydrogen abstraction from electron-donor species. The potential well (point D) corresponds to the electron-transfer intermediate. The dashed lines correspond to the primary natural state correlation.

involves overall β -CH cleavage of the amine, but it has been clearly established that an electron transfer is the first step of the process (3).¹⁰ To draw the MO natural correlation diagram, it is sufficient



(3)

to add the n_N lone-pair orbital of the nitrogen atom to the general diagram of Figure 4 for hydrogen abstraction from alkyl groups. One obtains the diagram of Figure 7. The interaction of the two lone pair n_N and n_R leads to the formation of two new orbitals which can be designed as π_{CN} and π^*_{CN} . The lowest states of the final system are the zwitterionic $1Z$ state, the diradical $1,3D_{\sigma\pi}$ and $1,3D'_{\sigma\pi}$ states. They are schematically represented in Figure 8. If one considers the following respective positions of the excited states of the initial system (GS, $1,3n_N\pi^*_{CO}$, $1,3n_O\pi^*_{CO}$) and of the final system ($1,3D_{\sigma\pi}$, $1Z$, $1,3D'_{\sigma\pi}$), one gets a state correlation diagram very similar to that of Figure 5c. Indeed, if one considers that the $n_N\pi^*_{CO}$ states are charge-transfer states, the diagram of Figure 8 and that of Figure 5c are exactly the same. There is a potential well which corresponds to a charge-separation intermediate. Thus the reaction can be analyzed as a two-step procedure. First, there is formation of an ion-pair intermediate (point D in Figure 9) after overcoming an energy barrier. Then the system decays to the lowest potential energy surfaces and reaches the $D_{\sigma\pi}$ states. These states correspond to the ground state of the intermediate which precedes the actual hydrogen-transfer

(9) Small energy barriers in the photoreactions of ketones are well established; see reference 4, p 237, 532.

(10) S. G. Cohen, A. Parola, and G. H. Parsons, Jr., *Chem. Rev.*, **73**, 141 (1973).

event. For overall hydrogen abstraction from amines, the electron transfer is generally more facile than in the most favorable cases of hydrogen abstraction from alkyl groups because, at one and the same time, the $n_N\pi^*_{CO}$ and $D'_{\sigma\pi}$ states are lower than the corresponding $\pi_{CO}\pi^*_{CC}$ and $Z'_{\sigma\pi}$ states.

Support for the qualitative correctness of the basic correlation diagrams given in Figures 5 and 6 is available from qualitative calculated potential energy curves.^{2a-c, 5b} For example, ab initio calculations^{5b} of hydrogen abstraction from methane by formaldehyde and of the α cleavage of acetone agree completely with the qualitative diagrams presented in this paper.

Conclusion

The four experimentally significant n-initiated photochemical reactions of ketones in their various manifestations can be analyzed in a unified manner with natural correlation diagrams which can be divided in two groups. There are those which involve the formation of a new σ bond on the ketonic framework: hydrogen abstraction from alkyl groups or amines and olefin addition. In such a case, the electronically allowed valence states are the $n_O\pi^*_{CO}$ states. If no low-lying charge-transfer states exist, the reaction involves direct formation of a diradical state throughout a single PEC with a potential barrier. If there is low-lying charge-transfer state, the reaction may be a two-step process, which involves in a first step the formation of an ion-pair inter-

mediate. It should be noted that the experimentally observed ion-pair intermediate could correspond to two situations. First, it may correspond to the potential well encountered on the PEC starting from the $n_O\pi^*_{CO}$ states in Figures 5 and 9, as already mentioned. Second it may correspond to the initial charge-transfer states ($n_N\pi^*_{CO}$, $\pi_{CC}\pi^*_{CO}$) which would have been populated by decay from the potential well corresponding to the first hypothesis. In this last hypothesis, the ion-pair intermediate has a long lifetime for the same reasons it cannot be directly populated. Thus, the subsequent hydrogen transfer or olefin addition would occur throughout a single surface linking the charge-transfer state to the ground state of the radical intermediate. Finally, there are the reactions which involve rupture of a σ bond that is α to the ketonic framework. In such a case, the electronically allowed reaction proceeds from the triplet $\pi_{CO}\pi^*_{CO}$, but reaction initiated from the $n_O\pi^*_{CO}$ states must be considered as possible pathways involving intersystem crossing or internal conversion. No charge-transfer state is possible and consequently cannot modify the general diagram in this case.

Acknowledgment. The authors at Columbia thank the National Science Foundation and the Air Force Office of Scientific Research for their generous support of this work. The authors at Paris acknowledge C.N.R.S. (Grant E.R.A. 549) for their generous support of this research.

Collision-Induced Dissociation Mass Spectrometry: Target Gas Effects upon Scattering and Charge Exchange

J. A. Laramée, D. Cameron, and R. G. Cooks*

Contribution from the Department of Chemistry, Purdue University, West Lafayette, Indiana 47907. Received May 27, 1980

Abstract: Collision-induced dissociation of polyatomic ions was studied with respect to the effects of ion and target mass and target ionization potential. Ionized argon, methane, and benzaldehyde were the projectiles, and a total of 24 target gases was examined. The relative importance of ion removal by scattering out of the collection angle of the detector, as opposed to removal by neutralization, was determined. Depending upon the target chosen, up to 40% of the initial ion beam could be neutralized and detected as unscattered fast neutrals. The cross section for neutralization showed an excellent inverse linear correlation to the ionization energy of the target. The loss of ion beam by scattering showed an approximate correlation with the mass of the target. The optimum conditions for collision-induced dissociation and charge exchange were investigated. Helium was found to be more effective than N_2 as a target for the dissociations of CH_4^+ , CH_5^+ , and $C_6H_5CHO^+$. In particular cases, up to 8% of the initial ion current could be collected as fragment ions.

Introduction

The effect of the target gas in high energy (keV) ion/molecule reactions of positive ions is studied as it pertains to the efficiency of collision-induced dissociation. This study is prompted by the growing use of collision-induced dissociation: in particular, its role in ion structural studies¹⁻¹³ and in the technique of mixture

analysis known as MIKES (mass-analyzed ion kinetic energy spectrometry) or ms/ms (mass spectrometry/mass spectrometry).¹⁴⁻¹⁶ The high-energy collision phenomena encountered here are also of interest for a number of other reasons. First, electron transfer leads to fast mass-selected molecular beams which are of use in pumped lasers and in fusion devices,¹⁷ second, electronic

(1) R. A. Yost and C. G. Enke, *J. Am. Chem. Soc.*, **100**, 2274 (1978); *Anal. Chem.*, **51**, 1251A (1979).

(2) K. R. Jennings, *Int. J. Mass Spectrom. Ion Phys.*, **1**, 227 (1968).

(3) K. Levsen and H. Schwarz, *Ang. Chem., Int. Ed. Engl.*, **15**, 509 (1976).

(4) D. L. Kemp and R. G. Cooks, "Collision Spectroscopy", R. G. Cooks, Ed., Plenum Press, New York, 1978.

(5) F. W. McLafferty, *Pure Appl. Chem.*, **50**, 831 (1978).

(6) S.-C. Tsai, Ph.D. Thesis, Cornell University, Ithaca, NY, 1972.

(7) F. W. McLafferty, P. F. Bente, III, R. Kornfeld, S.-C. Tsai, and I. Howe, *J. Am. Chem. Soc.*, **95**, 2120 (1973).

(8) F. W. McLafferty, R. Kornfeld, W. F. Haddon, K. Levsen, I. Sakai, P. F. Bente, III, S.-C. Tsai, and H. D. R. Schuddemage, *J. Am. Chem. Soc.*, **95**, 3886 (1973).

(9) K. Levsen and H. D. Beckey, *Org. Mass Spectrom.*, **9**, 570 (1974).

(10) T. Wachs and F. W. McLafferty, *Int. J. Mass Spectrom. Ion Phys.*, **23**, 243 (1977).

(11) M. S. Kim and F. W. McLafferty, *J. Phys. Chem.*, **82**, 501 (1978).

(12) C. J. Porter, R. P. Morgan, and J. H. Beynon, *Int. J. Mass Spectrom. Ion Phys.*, **28**, 321 (1978).

(13) R. P. Morgan, A. G. Brenton, and J. H. Beynon, *Int. J. Mass Spectrom. Ion Phys.*, **29**, 195 (1979).

(14) W. F. Haddon, *ACS Symp. Ser.*, No. 70 (1978).

(15) R. W. Kondrat and R. G. Cooks, *Anal. Chem.*, **50**, 81A (1978).

(16) F. W. McLafferty and F. M. Bockhoff, *Anal. Chem.*, **50**, 69 (1978).

(17) H. Winter, E. Bloemen, and F. J. deHeer, *J. Phys. B*, **10**, L453 (1977).